Eleventh International Conference on CFD in the Minerals and Process Industries
CSIRO, Melbourne, Australia
7-9 December 2015

HYDRODYNAMICS AND RADIATION EXTINCTION CHARACTERISTICS FOR A FREE FALLING SOLID PARTICLE RECEIVER

Apurv KUMAR[1*] and Jin-Soo KIM[1]

[1] CSIRO Energy Flagship, Newcastle, NSW 2290, AUSTRALIA

ABSTRACT

Free falling solid particle receivers are widely propagated solar receiver design due to its inherent functional simplicity. However, a low magnitude of operational thermal efficiency inhibits its utility in a high temperature Concentrated Solar Power (CSP) plant. The present paper numerically studies the hydrodynamics and attenuation characteristics to investigate the ambiguities in its design in order to improve it to increase the thermal efficiency of the high temperature particle receivers. CFD is utilised to solve the two dimensional free falling solid particle receivers and a parametric analysis is carried out. It is found that there is a scope of improvement in the residence time of the particles which could substantially impact the thermal efficiency of the receiver.

NOMENCLATURE

D	Particle size, m
I	Radiation intensity, W/m^2
p	Pressure, N/m^2
Q	Efficiency
R	Radius, m
Re	Reynolds no.
S	Distance/thickness of particulate media, m
T	Time, s
U,V	Velocity, m/s
x	Size parameter, 2πD/ λ
X,Y	Length, m
Greek letters	
β	Extinction coefficient, m^{-1}
ε	Porosity
λ	Wavelength, m
Φ	Transmissivity
ρ	Density, kg/m^3
μ	Dynamic viscosity, Pa s
Sub-scripts	
g	gas
p	solid
Ext	extinction
S,s	at distance S

INTRODUCTION

Solid particle receivers are currently being investigated worldwide (HO and IVERSON 2014) as an alternative to liquid metal and superheated CO_2 receivers due to its ability to reach very high temperature (around 1000 °C) and functional simplicity. Higher temperature coupled with higher solar flux are expected to play a major role in escalating the thermal efficiency of the particle receiver which could substantially impact the cost of power generation. Free falling particle receivers are the rudimentary designs in which a particle curtain is formed by freely falling particles through an aperture. Variants of

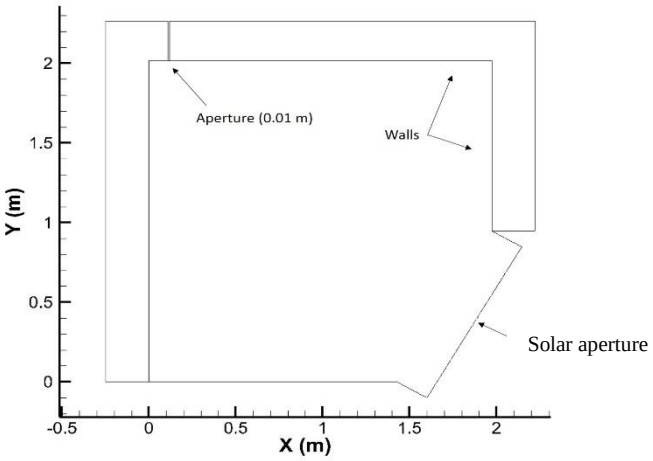

(a)

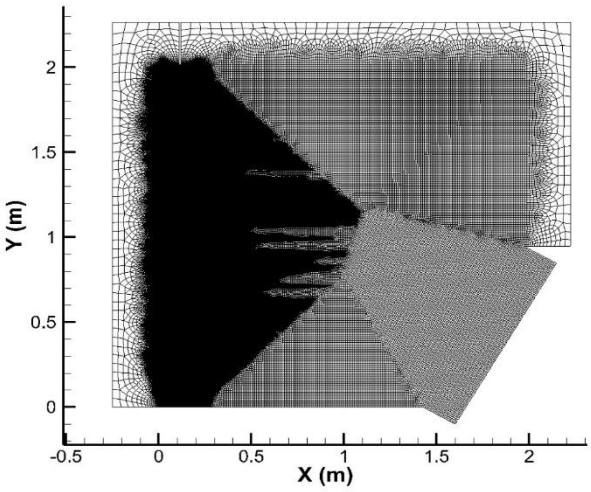

(b)

Figure 1: Geometry and computational model of the free falling particle receiver

this design are currently being investigated by researchers (RIGHTLEY, MATTHEWS et al. 1992, MEIER 1999, BAI, ZHANG et al. 2014, GOBEREIT, AMSBECK et al. 2015) to optimise and enhance the heat transfer and storage techniques. However, studies in relation to its utility for high temperature radiative heat transfer is limited. The present paper discusses the hydrodynamics characteristics and radiative properties of a freely falling solid particle receiver. A parametric analysis follows which could be utilised to enhance the thermal design. Use is made of commercial CFD program ANSYS FLUENT in order to numerically solve the solid-gas multiphase problem of a solid particle receiver geometry (Fig.1). An Eulerian-Eulerian multiphase model (Two fluid model) is used that assumes the solid and gas phase to be interpenetrating continuous media. Such solution models greatly reduce the computational time and are ideally suited for efficient study.

Two fluid model

Two-fluid model considers each of the phases to be interpenetrating continua and the governing equations of mass and momentum conservations are solved in ANSYS Fluent for each of the phases which are local mean averages of the point fluid and particles variables. Details on the derivation of the continuum equations for fluidized beds are provided by Gidaspow (1994) and several investigators. Thus, in the present study an isothermal Eulerian-Eulerian approximation is used with the particle phase limited to a constant diameter. In this model the necessary continuum equations for volume fraction and velocities are:

Continuity equations

Gas phase:

$$\frac{\partial(\varepsilon_g \rho_g)}{\partial t} + \nabla \cdot (\varepsilon_g \rho_g \overrightarrow{v_g}) = 0 \qquad (1a)$$

Solid phase

$$\frac{\partial(\varepsilon_p \rho_p)}{\partial t} + \nabla \cdot (\varepsilon_p \rho_p \overrightarrow{v_p}) = 0 \qquad (1b)$$

Momentum Equations

Gas phase

$$\frac{\partial(\varepsilon_g \rho_g \overrightarrow{v_g})}{\partial t} + \nabla \cdot (\varepsilon_g \rho_g \overrightarrow{v_g} \overrightarrow{v_g}) = -\varepsilon_g \nabla P_g + \nabla \cdot \tau_g + \beta_{gs}(\overrightarrow{v_g} - \overrightarrow{v_s}) + \varepsilon_g \rho_g \vec{g} \qquad (2a)$$

Solid phase

$$\frac{\partial(\varepsilon_p \rho_p \overrightarrow{v_p})}{\partial t} + \nabla \cdot (\varepsilon_p \rho_p \overrightarrow{v_p} \overrightarrow{v_p}) = -\varepsilon_p \nabla P_g - \nabla P_p + \nabla \cdot \tau_p - \beta_{pg}(\overrightarrow{v_g} - \overrightarrow{v_p}) + \varepsilon_p \rho_p \vec{g} \qquad (2b)$$

Where

$$\tau_g = \mu_g\left[\nabla \overrightarrow{v_g} + \nabla^{\mathrm{T}} \overrightarrow{v_g}\right] - \frac{2}{3}\mu_g(\nabla \cdot \overrightarrow{v_g})\boldsymbol{I} \qquad (3a)$$

$$\tau_p = \mu_s\left[\nabla \overrightarrow{v_p} + \nabla^{\mathrm{T}} \overrightarrow{v_s}\right] + \left(\pi_p - \frac{2}{3}\mu_p\right)(\nabla \cdot \overrightarrow{v_p})\boldsymbol{I} \qquad (3b)$$

and $\varepsilon_p + \varepsilon_p = 1$

For the problem to be completely defined the governing equations require closures for the solid-phase pressure (P_p), solid phase shear viscosity (μ_p) and the solid-phase bulk viscosity (π_p). These constitutive equations are derived from kinetic theory of granular flow (KUMAR, HODGSON et al. 2012). Apart from these closures, kinetic theory of granular flow requires the solution to transport equation for the granular temperature. Granular temperature, Θ, signifies the random motion of the solid particles and is analogous to temperature definition according to the kinetic theory .

$$\frac{3}{2}\left[\frac{\partial(\varepsilon_s \rho_s \Theta_s)}{\partial t} + \varepsilon_s \rho_s \overrightarrow{v_s} \Theta_s\right] = (-P_s \boldsymbol{I} + \tau_s) : \nabla \overrightarrow{v_s} + \nabla \cdot (k_s \nabla \Theta_s) - \gamma + \phi_s \qquad (4)$$

Drag laws

Coupling between the solid and fluid phase in Two-fluid model is through the interphase momentum exchange coefficient, F_s. In literature, several semi-empirically closures are presented in order to define F_s. Of these, the Gidaspow model (1994) (eq.5) is the widely used drag law and is a combination of drag law by Ergun (1952) and Wen and Yu (1966).

$$F_s = 150\frac{(1-\varepsilon_g)^2 \mu_g}{\varepsilon_g {d_s}^2} + 1.75\frac{\rho_g(1-\varepsilon_g)(\overrightarrow{v_g} - \overrightarrow{v_s})}{d_s} \quad for\ \varepsilon_g \le 0.8 \qquad (5a)$$

$$F_s = \frac{3}{4}C_D\frac{(1-\varepsilon_g)\varepsilon_g \rho_g(\overrightarrow{v_g} - \overrightarrow{v_s})}{d_s}\varepsilon_g^{-2.65} \quad for\ \varepsilon_g > 0.8 \qquad (5b)$$

where $C_D = \frac{24}{\varepsilon_g Re_g}\left[1 + 0.15(\varepsilon_g Re_g)^{0.687}\right]$

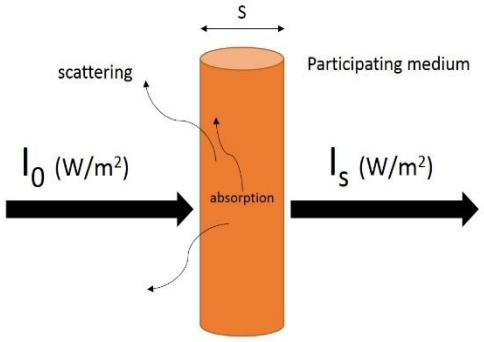

Figure 2: Radiation attenuation by a participating medium

RADIATIVE PROPERTIES OF PARTICULATE MEDIA

Particle receivers form a cloud of particles which absorb or scatter the incident radiation. Parameters such as particle size, shape, refractive index, porosity of particulate media etc. effect the scattering and absorption of radiation (MODEST 2003). Therefore, the transmissivity of a particulate cloud greatly depends on its attenuation properties and is of great importance to obtain the optimum design of receivers.

For independent scattering ($c/\lambda >> 1$) (MODEST 2003), the extinction coefficient, $\beta = (\kappa + \sigma)$ where, κ is the absorption coefficient and σ is the scattering coefficient. It is also known (MODEST 2003),

$$\beta = Q_{ext}\frac{(1-\varepsilon)}{\varepsilon}\frac{3}{4r} \qquad (6)$$

Where, Q_{ext} is the extinction efficiency and Q~2 for $x \to \infty$

The loss of radiation intensity through a particulate media of thickness, S, can be summarised as (Fig. 2) :

$$\frac{I_s}{I_0} = e^{\int_0^S -\beta(S)dS} \quad (7)$$

Transmissivity (Φ) is therefore defined as:

$$\Phi = \frac{I_s}{I_0} \quad (8)$$

PROBLEM DESCRIPTION

An unsteady two dimensional solid-gas multiphase flow model is solved numerically using the Two fluid model in ANSYS FLUENT v15. The freely falling particle receiver is 2m long with a window to allow solar radiation from the heliostat field at an angle of 120° from horizontal. An aperture at the top (0.01m) is used to release the stream of particles. CARBO HSP particles are used in the present case (Table 1). The numerical model is validated using published data for solid volume fraction along the centreline of the curtain (KIM, SIEGEL et al. 2009) (Fig.3). A mesh independent study was carried out and optimum no. of elements (160,000) were selected for all numerical

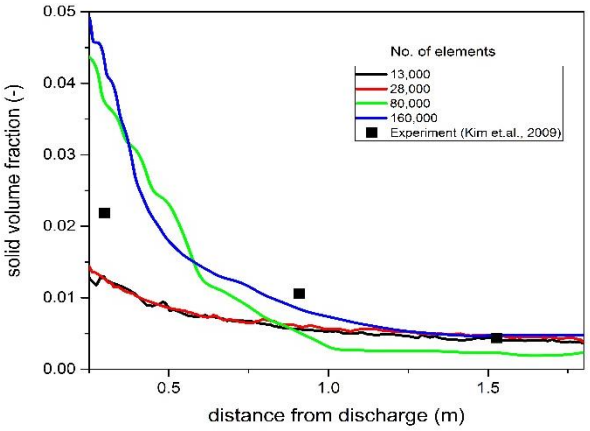

Figure 3: Grid independent study and validation of the numerical model with experiments (Kim et al.,2009)

solution (Fig.3). A time step of 0.5ms was used for stable and accurate results.

Parametric study was carried out to study the hydrodynamics and attenuation characteristics. Effect of mass flowrate of the particles through the aperture and the particle diameter on the particle velocity, solid volume fraction and the extinction coefficient were investigated.

The extinction coefficient, β is calculated assuming an incident radiation beam in intercepted by the falling particles at an angle of 120° originating from the solar window. The thickness of the particulate media (S) is divided into 1000 segments and extinction coefficient is calculated for each of these segments for an incident beam. Fig.4 depicts the location, angle and direction of the calculations carried out after the numerical solution is completed. The transmissivity for each selected segment can be calculated from Eq.8 for a given extinction coefficient.

RESULTS AND DISCUSSION

Effect of mass flowrate

The mass flowrate of the falling particles was varied from 3 to 9 kg/s (for 1000μm) without varying the aperture width. Figure 5 shows the velocity of the particles at different location from the discharge point along the axis of the aperture. The particle velocity monotonically increases until terminal velocity is reached. The effect of mass flowrate of particle is seen to be minimal on the magnitude

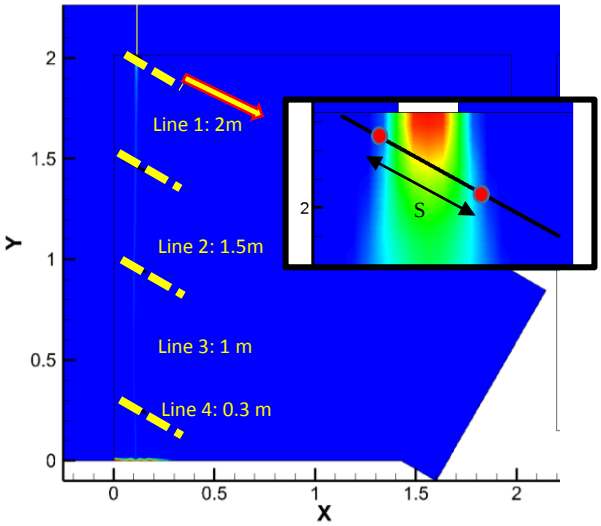

Figure 4 : Description of the methodology to calculate the extinction coefficient and transmissivity of the particle cloud (thickness, S) (Inset: Solid fraction contour plot showing particle cloud thickness, S)

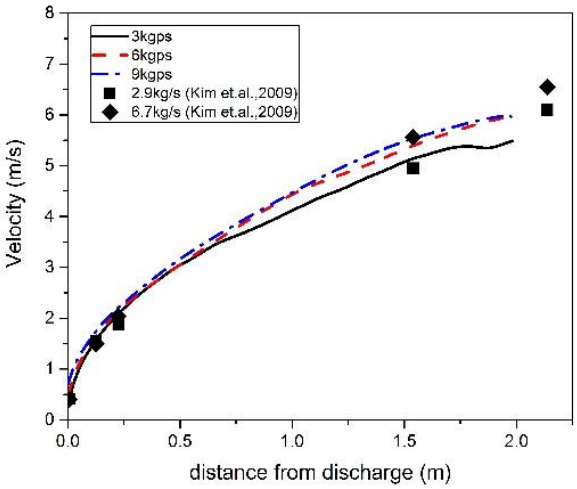

Figure 5: Effect of mass flowrate on the particle velocity along central axis for 1000μm particle size

Table 1: Solid particle physical properties

Material composition (CARBO HSP)	Alumina silicate (~7% Fe_2O_3)
Specific gravity	3.56
Bulk density (g/cc)	2

of velocity along the central axis. Velocities as high as 6-7 m/s are reached by the particles which denotes a very small residence time (inverse of particle velocity) of the particles. This is disadvantageous for solar radiation heat

transfer as ideally it is favourable for particles to remain in the cavity for a longer time to ensure complete absorption of solar energy.

locations (2, 1.5, 1 and 0.3 m from the bottom of the receiver). Line 1 is of shorter length due to its location just adjacent to the top wall. It can be seen that the particle cloud is made of two regions, a core and an exterior region. The core is relatively more opaque than the exterior region and

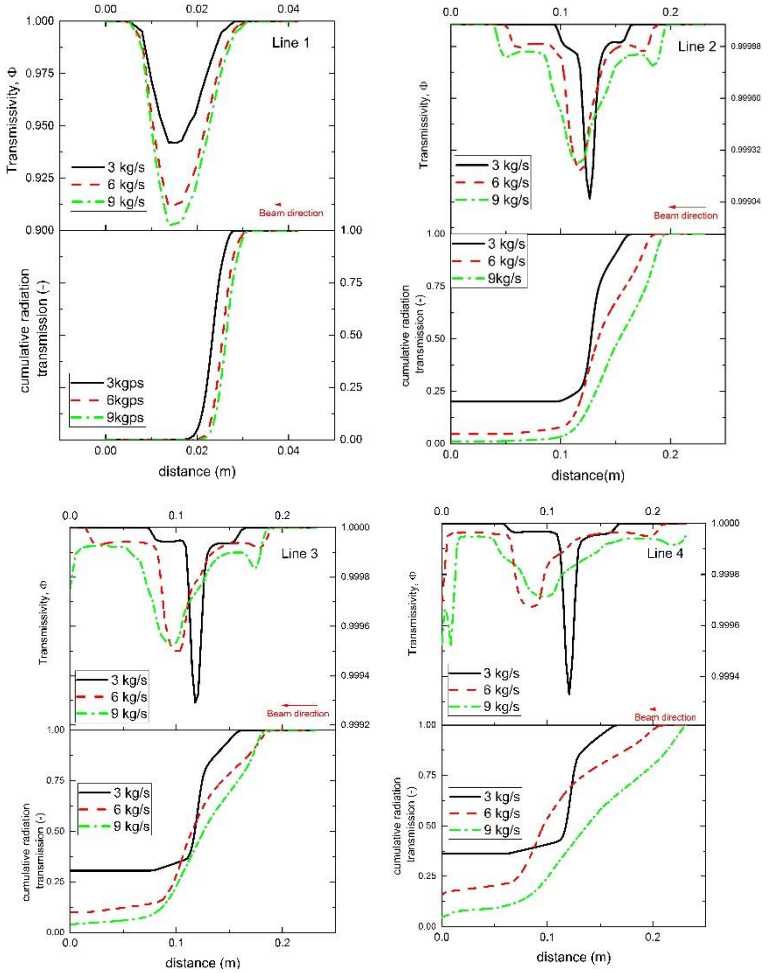

Figure 6: Effect of mass flowrate on transmissivity and the cumulative transmission of incident radiation through the particle cloud at various location from discharge. (NB: The beam direction is from right to left)

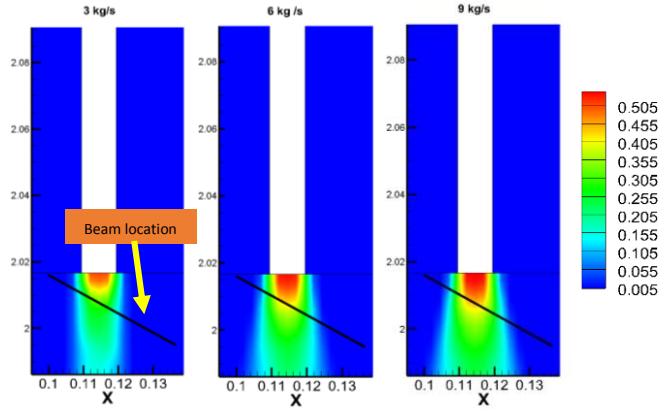

Figure 7: Volume fraction contour for different flowrates at the discharge location (the black line is the beam location)

Figure 6 plots the effect of mass flow rate on the transmissivity of the particle cloud and the cumulative transmission of the incident radiation at 4 different

major of the incident beam gets absorbed in the core. The transmissivity plot denotes a segment wise analysis of the cloud. A cumulative transmission plot reveals how much radiation is allowed by the cloud to hit the wall.

With increasing mass flowrate, the maximum core transmissivity of the particle cloud decreases except for Line 1, which is located just below the aperture. Figure 7 shows the solid volume fraction contours. For 3 kg/s, the core is smaller than for other flowrates due to which the incident beam is transmitted to a greater degree than for other flowrates. Other beam locations (Line 2-4) show a decreasing trend of transmissivity with increase of mass-flowrate. Along with decrease of transmissivity with increasing mass flowrate, the cloud thickness also increases. Due to the combined effect, the total attenuation of the incident beam increases with increasing mass flowrate. As high as 40% of incident beam escapes the particle cloud (Line 4; 3kg/s) which shows that a design modification is needed to reduce radiation loss in falling particle receivers. A good design must be able to reduce the radiation loss to an acceptable limit.

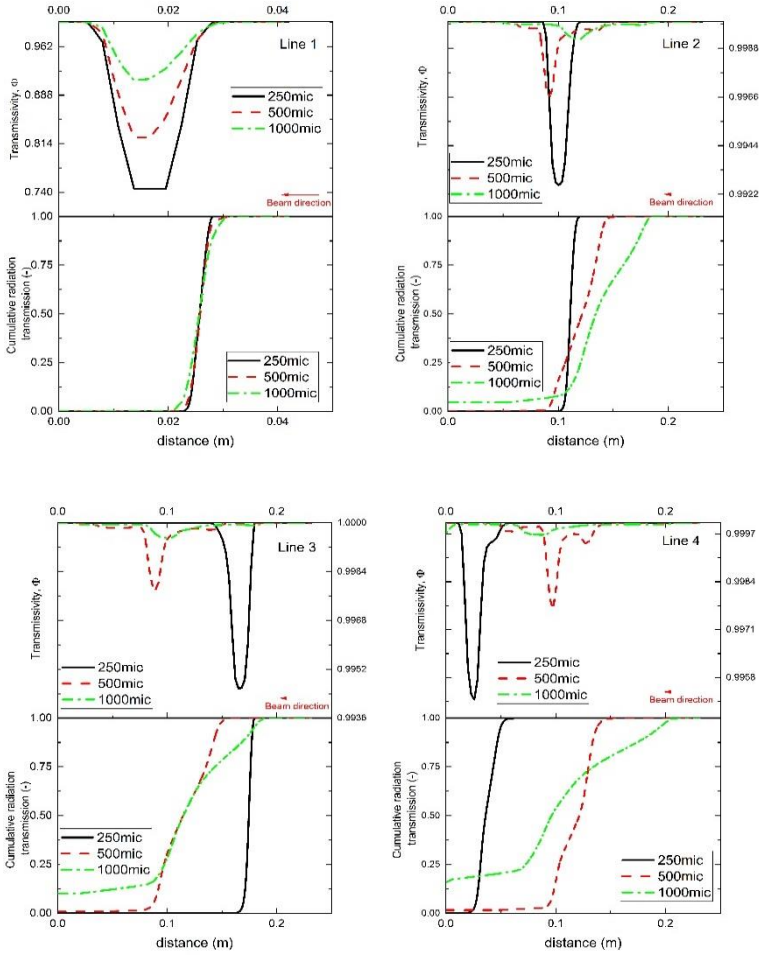

Figure 8: Effect of particle diameter on transmissivity and the cumulative transmission of incident radiation through the particle cloud at various location from discharge. (NB: The beam direction is from right to left)

Effect of particle diameter

Figure 8 plots the variation of transmissivity for different particle diameters. The post analysis was carried out on mass flowrate of 6kg/s and 500μm particles. It is seen from the figure that the cloud transmissivity increases with increasing particle diameter. In addition, the cloud thickness is seen to increase with increasing particle size. The exit cumulative transmissivity is thus seen to increase with increasing particle size. Finer particles cloud maintained their opacity till the bottom of the receiver as opposed to coarser particles which became transparent and had a wide cloud thickness. The trajectory of finer particles cloud diverted to a greater degree than the coarse particles. This is the reason why the transmissivity in Figure 8 for line 3 and 4 is seen to fluctuate at the left wall (distance = 0).

An alternative to improve the transmissivity issue of the particle cloud can be to reduce the particle diameter as it greatly reduces the transmissivity of the particle cloud. However, reducing the particle diameter can alter the hydrodynamics of the particle cloud, for instance, a wavy trajectory. This may lead to further issues with particle entrainment which possess practical difficulty in operating a particle receiver. As seen from the cumulative radiation transmission plots (Fig.6 and 8), approximately more than 90% of the radiation is absorbed by the first half of the cloud thickness. This means that the required effective thickness of the cloud that would participate in heat transfer is less than what free falling receiver is offering. There is scope to design a receiver with a reduced cloud thickness without affecting the radiation characteristics.

CONLCUSION

A two dimensional unsteady solid-gas multiphase flow was numerically solved to estimate the hydrodynamics and radiation attenuation characteristics of a free falling solar particle receiver. The study intended to understand the specific areas of design improvement to enhance the thermal efficiency of the particle receiver. It was found that:

a) The particle velocity is a critical parameter that can be reduced to enhance the absorption of the radiation by the particle cloud.
b) Maximum of radiation attenuation takes place by approximately half of the cloud thickness in the range of particle size and flow rate of this study. A good receiver could be designed with a reduced cloud spread.
c) Reducing particle size helps in improving the radiation properties of the particle cloud but has detrimental effects on the cloud trajectory which can enhance particle entrainment.

It is imperative to bring essential changes to the geometry of a solar particle receiver in order to obtain improved and optimized thermal performance. A novel design concept is

being pursued to enhance the thermal efficiency of the particle receiver.

ACKNOWLEDGEMENTS

This research was performed as part of the Australian Solar Thermal Research Initiative (ASTRI), a project supported by the Australian Government, through the Australian Renewable Energy Agency (ARENA).

REFERENCES

BAI, F., Y. ZHANG, X. ZHANG, F. WANG, Y. WANG and Z. WANG (2014). "Thermal Performance of a Quartz Tube Solid Particle Air Receiver." Energy Procedia **49**: 284-294.

ERGUN, S. (1952). "Fluid Flow through Packed Coloumns." Chemical Engineering Progress **48**(2): 89-94.

GIDASPOW, D. (1994). Multiphase Flow and Fluidisation, Academic Press, San Diego.

GOBEREIT, B., L. AMSBECK, R. BUCK, R. PITZ-PAAL, M. ROEGER and H. MUELLER-STEINHAGEN (2015). "Assessment of a falling solid particle receiver with numerical simulation." Solar Energy **115**: 505-517.

HO, C. K. and B. D. IVERSON (2014). "Review of high-temperature central receiver designs for concentrating solar power." Renewable & Sustainable Energy Reviews **29**: 835-846.

KIM, K., N. SIEGEL, G. KOLB, V. RANGASWAMY and S. F. MOUJAES (2009). "A study of solid particle flow characterization in solar particle receiver." Solar Energy **83**(10): 1784-1793.

KUMAR, A., P. HODGSON, D. FABIJANIC and W. GAO (2012). "Numerical solution of gas–solid flow in fluidised bed at sub-atmospheric pressures." Advanced Powder Technology **23**(4): 485-492.

MEIER, A. (1999). "A predictive CFD model for a falling particle receiver reactor exposed to concentrated sunlight." Chemical Engineering Science **54**(13-14): 2899-2905.

MODEST, M. F. (2003). Chapter 12 - Radiative Properties of Semitransparent Media. Radiative Heat Transfer (Second Edition). M. F. Modest. Burlington, Academic Press**:** 413-422.

RIGHTLEY, M. J., L. K. MATTHEWS and G. P. MULHOLLAND (1992). "Experimental characterization of the heat-transfer in a free-falling-particle receiver." Solar Energy **48**(6): 363-374.

WEN, C. Y. and Y. H. YU (1966). "Mechanics of Fluidisation." Chenmical Engineering progress symposium series **62**: 100.

